COMPARISON OF MEASURED AND COMPUTED ULTIMATE STRENGTHS OF FOUR HIGHWAY BRIDGES

Edwin G. Burdette and David W. Goodpasture, Department of Civil Engineering, University of Tennessee

Four deck girder highway bridges in Tennessee, located in an area to be flooded as a part of a TVA reservoir, were tested to failure under static loading. The ultimate load for each bridge, defined as the maximum load-carrying capacity of the bridge, was measured. This measured load was compared to loads that were computed by strain compatibility relations in which actual stress-strain properties of the materials were used and the entire bridge including curbs was assumed to act as a wide beam spanning between supports, and by the 1971 Interim Specifications of AASHO, in which the capacities of all girders were summed. In both methods, a flexural mode of failure was assumed. Also, the load causing first permanent set was computed and compared with the measured load. The analytical method based on strain compatibility predicted the ultimate capacity of 3 of the bridges within 9 percent. Each bridge failed in a flexural mode. Composite action was lost in the prestressed concrete bridge prior to flexural failure, with a resulting reduced load capacity. The loads based on AASHO Specifications gave a lower bound to the actual ultimate loads for each bridge. The load causing first permanent set is less readily identifiable, either theoretically or experimentally, than is the ultimate load. The method given in the AASHO Specifications for limiting overload on the basis of first permanent set appears reasonable.

•FOUR deck girder highway bridges, located in Franklin County, Tennessee, were tested to failure during the summer of 1970. These bridges were located in an area that has since been flooded as a part of the Tennessee Valley Authority's Tims Ford Reservoir and were made available by the Tennessee Highway Department and TVA for testing purposes. The testing was performed as a part of a research contract between the Civil Engineering Department of the University of Tennessee and the Tennessee Department of Highways in cooperation with the Federal Highway Administration. A complete description of the testing program and a compilation of the test results are given in the final report for the research project (1).

The apparent trend in the Specifications of the American Association of State Highway Officials is toward the use of "load factor design" for deck girder bridges. This design philosophy is based on the prediction of ultimate capacity of the individual bridge girders along with considerations of the amount of overload that would cause first permanent set and fatigue considerations. The research reported in this paper represents a unique opportunity to assess, through tests on typical highway bridges, the accuracy with which the bridge designer is able to predict ultimate bridge capacity and load causing first permanent set.

The primary objective of this paper is to compare the computed and measured ultimate strengths of each of the 4 bridges. Two values of computed ultimate capacity were obtained for each bridge: (a) The ultimate bridge capacity was determined by summing the ultimate capacities of each longitudinal girder in the bridge, as calculated on the basis of the 1971 Interim Specifications of AASHO (2); and (b) the capacity of each bridge was calculated on the basis of strain compatibility relations, using the actual stress-strain relations of the material in the structure. In the latter method the entire bridge, with curbs, was considered to act as a unit. In both methods, ultimate capacity was assumed to be controlled by the flexural strength of the bridges.

A secondary objective is to compare the theoretically calculated load causing first permanent set for each bridge with the value obtained from experimental load-deflection curves for the bridge. The behavior and mode of failure of each bridge, as observed in the tests, are described and discussed.

DESCRIPTION OF BRIDGES

Each of the four bridges was a 2-lane deck girder bridge with 4 longitudinal girders. A description of the bridges is given in Table 1, and photographs of the bridges are shown in Figure 1.

From a testing viewpoint, bridges 1 and 4 were the most useful of the 4 bridges. Bridge 1 was on a flat sag vertical curve; in all other respects these 2 bridges were ideal for testing: 90-deg skew, horizontal tangent, almost 0 grade, and recent construction.

Bridge 2, composed of AASHO type 3 precast, prestressed sections, was also of recent design and was a widely used type. Its usefulness as a test specimen, however, was limited somewhat by the presence of a 70-deg skew, a grade of approximately 4½ percent, and a superelevated roadway because of a 4½-deg horizontal curve. Although bridge 3 was not of recent design and had a 60-deg skew, it had a 0 grade and was not curved. Also, the reinforced concrete T-beam construction is representative of a number of bridges currently in use throughout the United States.

COMPUTATIONS

The ultimate load-carrying capacity of a bridge subjected to flexural loading depends not only on its own flexural capacity but also on the position of the applied loads. The position of the loads in the actual tests to failure is described in detail at a later point in this paper. For the tests, the loads were placed in such a way as to simulate an HS loading in the position resulting in maximum positive moment near the center of a span. It was that load position for each bridge that was used in the calculations to predict ultimate load-carrying capacity. The loads were assumed, for calculation purposes, to have uniform lateral distribution; that is, the loads were treated as line loads extending across the bridge deck.

All values given for maximum load-carrying capacity refer to applied live load. The moment due to dead load was subtracted from the total moment capacity prior to calculation of maximum load.

Theoretical Ultimate Capacity

The ultimate load capacity of each bridge was calculated on the basis of strain compatibility relations that considered the actual stress-strain properties of the steel and ultimate compressive strength of the concrete in each bridge. The stress-strain curves are shown in Figure 2. The average ultimate compressive strength of the concrete in the bridge decks for each bridge, obtained from cores, is given in Table 2. The coefficients given in the ACI Code (3) were used to define the concrete stress block in compression.

In the determination of theoretical ultimate capacity, each bridge was assumed to act as a unit, with the curbs acting as an integral part of the unit. Any effect of handrails was neglected.

The method used to calculate the ultimate moment capacity at both positive and negative moment sections of bridge 4 and the negative moment sections of bridge 1 was simply that of multiplying the experimentally determined yield stress of the steel by the plastic modulus. The determination of ultimate moment capacity at positive moment sections in bridges 1, 2, and 3 involved consideration of both concrete and steel; the method used required the application of 3 necessary relationships: equilibrium of horizontal forces and moments, assumption of linear strain distribution, and knowledge of the stress-strain relations for concrete and steel. The method of analysis, particularly as applied to prestressed concrete beams, is described in detail elsewhere (4, 5).

Once the ultimate moment capacity was calculated for simple-span bridges 2 and 3, the determination of ultimate load consisted of calculating the applied load that, acting

Table 1. Description of bridges.

Number	General Description	Span (ft)	Girder Spacing		Skew (deg)	Location	Design Loading and Date
			Feet	Inches			
1	4-span continuous, 36-in. steel rolled beams, composite in positive moment regions	70, 90, 90, 70	8	4	90	Tenn-130 over Elk River	HS-20, 1963
2	Simple span composite with AASHO type 3 precast, prestressed concrete beams	66	8	10[a]	70	Tenn-130 over Boiling Fork Creek	HS-20, 1963
3	Simple span reinforced concrete T-beams, monolithic construction	50	6	10	60	US-41A over Elk River	H-15, 1938
4	3-span continuous, noncomposite, 27-in. steel rolled beams	45, 60, 45	7	4	90	Mansford Road over Elk River	H-15, 1956

[a]Varies because of 4½-deg horizontal curve.

Figure 1. Test bridges.

Bridge 1

Bridge 2

Bridge 3

Bridge 4

Table 2. Measured and computed results.

Bridge	Avg Ultimate Compressive Strength (psi)	Ultimate Load			Centerline Deflection (in.)	Load Causing First Permanent Set		
		Measured (kip)	Theoretical (kip)	AASHO (kip)		Measured (kip)	Computed (kip)	Permanent Deflection (in.)
1	6,800	1,250	1,270	930	22.8	620	714	0.25
2	5,500	1,140	1,267	1,100	9.5	660	759	0.12
3	6,500	1,580	1,465	844	7.2	—	—	—
4	5,600	640	696	388	26.4	500	376	0.00

in combination with the existing dead load, would produce the calculated ultimate moment. For continuous bridges 1 and 4, a "limit analysis" was made in which redistribution of moments after yielding was considered. Figure 3 shows the position of the applied loads on the loaded span for each bridge and the magnitudes of the calculated ultimate moments. The end moment at the pier at the left of the span for bridge 1 is that caused by dead load only, because there was no provision at the left abutment for resisting an upward reaction, and the load causing failure was large enough to cause the bridge to lift off the abutment. The theoretically calculated ultimate loads are given in Table 2.

Ultimate Capacity Predicted From AASHO Specifications

The 1971 Interim Specifications of AASHO (2) were used as a basis for calculation of the ultimate capacity of bridges 1, 2, and 4. These specifications do not provide for the determination of ultimate capacity of reinforced concrete bridges such as bridge 3. Thus, the AASHO Specifications' value of ultimate capacity for bridge 3 was calculated by using the general method presented for determination of flexural capacity in the ACI Code (3); this method is believed to hold to the "spirit" of the 1971 AASHO Interim Specifications. The ultimate loads calculated by the AASHO Specifications are given in Table 2.

Bridge 1—The concrete and steel properties for this bridge were taken as $f_c' = 6{,}000$ psi and ASTM A-36 respectively. The ultimate positive moment capacity near the center of the span, based on composite design, was calculated to be 13,600 kip-ft. This value was obtained by summing the flexural capacities of all 4 girders. The position of the loads was such that, when the ultimate moment was reached near the center of the span, the sections at the supports were still elastic. The Specifications make no provision for limit behavior; therefore, the maximum load was calculated as that which produced the ultimate moment near the center of the loaded span. A computer analysis of the structure was carried out through the use of ICES STRUDL-II and took account of the nonprismatic bridge cross section. The maximum load-carrying capacity was calculated on this basis to be 930 kips.

Bridge 2—The concrete and steel properties for this simple-span bridge were taken as $f_c' = 5{,}500$ psi and $f_s' = 250$ ksi respectively. The 4 AASHO-PCI type 3 precast girders were assumed to act compositely. The ultimate moment capacity for the entire bridge was calculated on the basis of the AASHO Specifications to be 17,400 kip-ft, and the maximum load-carrying capacity was calculated to be 1,100 kips.

Bridge 3—The concrete and reinforcing steel properties for this simple-span bridge were taken as $f_c' = 4{,}500$ psi (limited by AASHO Specifications, section 1.5.1B) and $f_y' = 40{,}000$ psi. The ultimate moment capacity was calculated to be 9,660 kip-ft, and the maximum load-carrying capacity, 844 kips.

Bridge 4—The steel in this noncomposite, 3-span continuous bridge was assumed to be A-36. The loads were placed on the span such that, when the plastic moment was reached near the center of the center span, the sections at the piers were still elastic. The total plastic moment for the bridge was calculated to be 3,500 kip-ft. The maximum load-carrying capacity was calculated, on the same basis as that described for bridge 1, to be 388 kips.

Calculation of Load Causing First Permanent Set

The 1971 AASHO Interim Specifications (2) attempt to ensure that permanent deformation will not occur under a specified overload by limiting the moment caused by dead load plus an amplified live load with impact to 95 percent of that causing first yield. For comparisons discussed later in this paper, the load producing first yield of the steel in bridges 1, 3, and 4 was calculated and is given in Table 2. The calculations were based on the experimentally determined yield strength of the steel in each bridge, and elastic theory was used.

Figure 2. Stress-strain curves for steel.

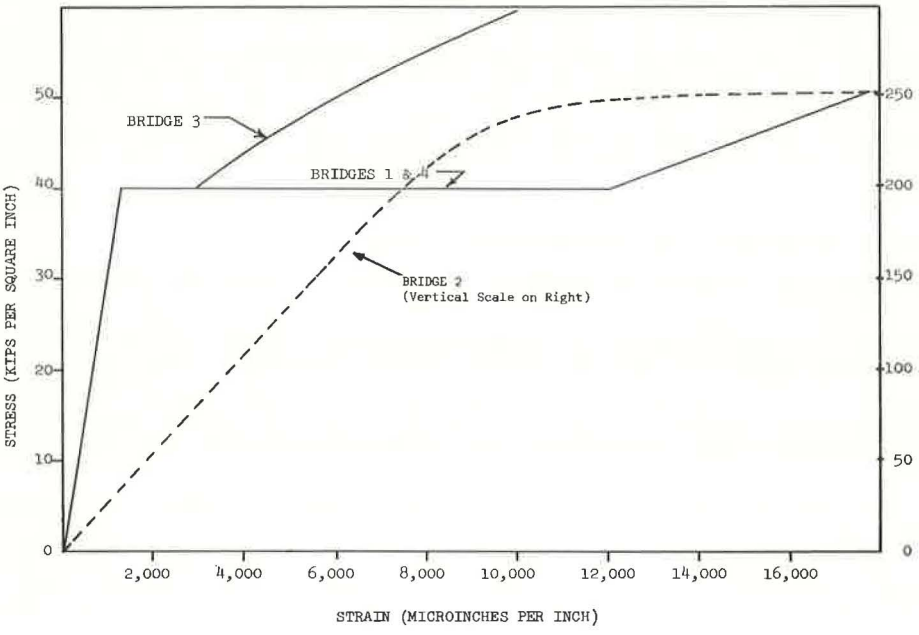

Figure 3. Location of applied loads and magnitudes of calculated ultimate moments (M* for bridge 1 = maximum moment that could be developed at first pier because of dead load only).

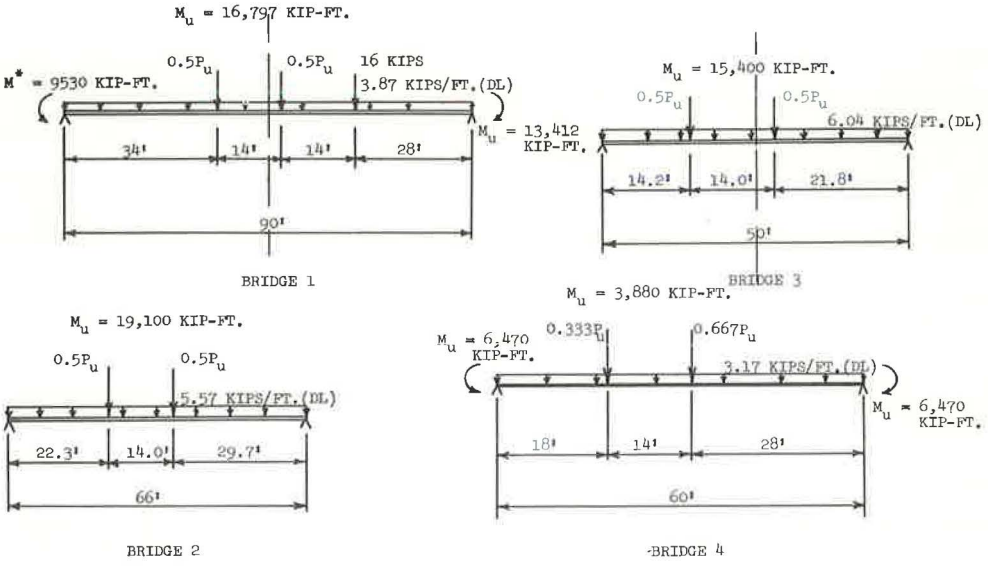

TEST PROCEDURE

Placement of Loads

The loads were placed on each bridge with the exception of bridge 4 in such a way as to simulate an HS truck located in each lane to cause maximum positive moment near the center of the span. The points on the span at which load was applied were at the positions of the 8 rear wheels of the 2 simulated trucks. For the test to failure of bridge 1, the 4 front wheels were simulated by four 4,000-lb pallets of concrete blocks. The simulation of front wheels was omitted for the other bridges. The positions of the applied loads for the 4 bridges are shown in Figure 4. Because of difficulties in rock drilling, only 6 load points were used for bridge 4.

Application of Load

The rather large loads required to cause bridge failure were developed through a "rock anchor system" and were applied to the bridge deck through a "bearing grill."

Rock Anchor System—At each of the 8 load points for each span, a hole was drilled through the concrete bridge deck. Directly below each one of these holes, a hole was drilled approximately 25 ft into the limestone rock, and an 18s reinforcing bar was grouted into place in this hole. The bar was terminated below the bridge deck, and a connection accommodating a $1\frac{3}{8}$-in. diameter Stressteel bar was welded to the top end of the 18s bar. After completion of all rolling load and other tests on each bridge, a $1\frac{3}{8}$-in. diameter Stressteel bar was connected to each of the 18s bars. The Stressteel bar extended through the hole in the bridge deck and through a 100-ton capacity center-hole jack, which rested on a bearing grill.

Bearing Grill—The bearing grill consisted of two 14-in. wide flange beams, 3 ft 10 in. long, spaced 2 ft 6 in. center-to-center. These beams were joined at the ends by two 12-in. channels, which spanned between the beams and were welded to the beams so that the bottom flanges of the channels were flush with the bottom surfaces of the beams in order to obtain uniform bearing. Two more channels spanned between the beams at the center of their 3-ft 10-in. length and were fastened to the beam webs. The load was applied by the hydraulic rams through a 2-in. thick steel bearing plate to these center channels. Soft wood two-by-tens were placed under the beams and on the bridge deck, and two-by-fours were placed under the end channels in order to minimize stress concentrations and reduce the likelihood of punching shear. In addition, it was necessary to cast concrete bearing pads on superelevated bridge 2 in order to apply the loads to a horizontal surface.

Loading Procedure

The load was applied to each load point by a Stressteel center-hole ram acting on a bearing grill. The rams were activated by an electric pump equipped with a pressure gauge that had a maximum capacity of 10,000 psi. The loads were applied in increments of 1,000 psi to near yielding and then in increments of 500 psi to failure. The force in each bar was obtained from strain readings after each increment of load. Also, strains at various points in the bridge were monitored, and level rod readings at several points on the bridge deck were taken after each load increment. The tests were discontinued at some point after the ultimate load of the bridges was attained. Ultimate load is defined as the maximum load attained in a test to failure, and failure is said to have occurred when an increase in deflection of the bridge takes place under a decreasing load.

TEST RESULTS

Behavior Mode of Failure

Each of the 4 bridges, with the exception of bridge 2, failed in a flexural mode, and each bridge behaved in a ductile manner. Load-deflection curves for one point near the centerline of the span on each bridge are shown in Figure 5; modes of failure are shown in Figure 6.

Figure 4. Position of loads used in tests.

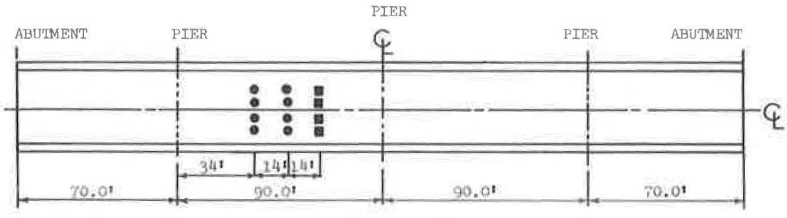

BRIDGE 1

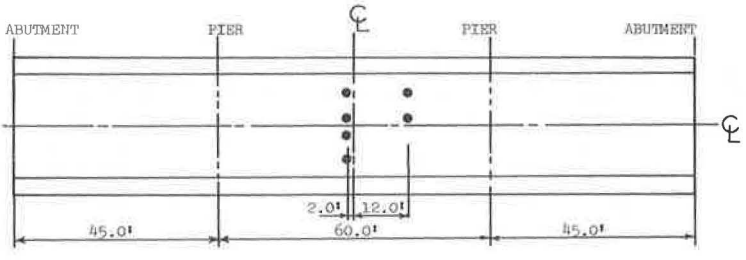

BRIDGE 4

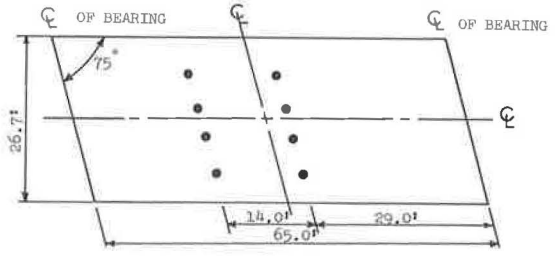

BRIDGE 2

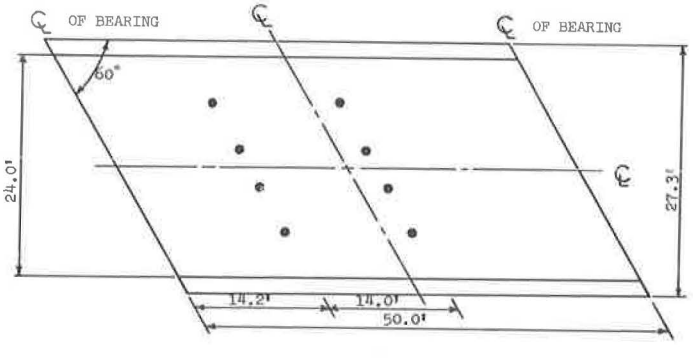

BRIDGE 3

● LOAD POINT

■ 4 KIP LOAD

Figure 5. Load-deflection curves.

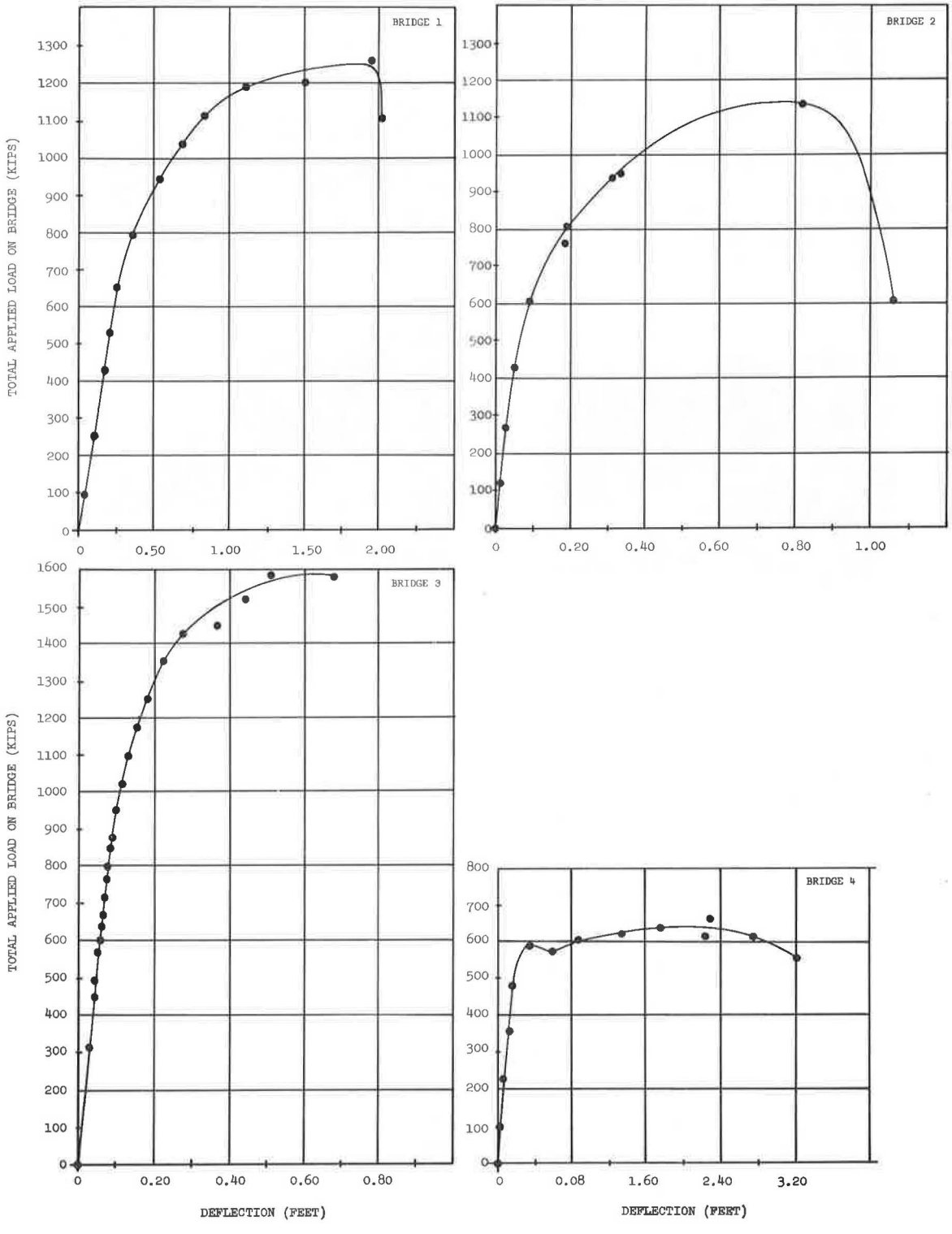

Figure 6. Mode of failure.

Bridge 1

Bridge 2

Bridge 4

Figure 7. Measured and computed ultimate loads.

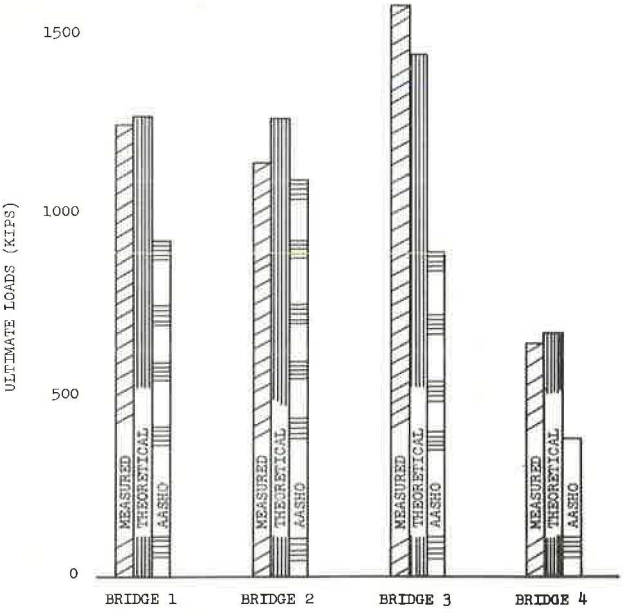

Bridge 1—The behavior of this bridge was almost linearly elastic up to yielding at the section under the applied loads nearest the center of the span. As the load was increased, there was considerable rotation at this section and, in turn, considerable deflection. Shortly after yielding began and the load was increased further, the bridge "lifted off" the abutment nearest the applied load, thus making it impossible to develop more moment at the first pier. The bridge continued to experience increasingly large deflections for each load increment until, after a very large deflection, yielding occurred, and a plastic hinge formed at a section near the center pier at the end of the cover plates on the side of the pier away from the loaded span. Shortly after this hinge formed, a secondary compression failure of one of the curbs occurred at the section of maximum positive moment, and the test was terminated.

Bridge 2—This bridge behaved in a predictable way up to a load of approximately 950 kips. However, there was considerable "dishing" of the bridge at this point, and the interior girders were deflected considerably more than the exterior girders. The result of this dishing was a tendency for the bridge deck to separate from the interior precast girders. At a load of approximately 950 kips this separation occurred, and composite action of the interior girders was lost as the vertical stirrups crossing the interface between girder and deck were sheared. After composite action was lost, the behavior of the bridge was radically changed. Almost immediately there was crushing of the extreme top fibers of the interior precast sections at the section of maximum moment. This crushing and accompanying rotation resulted in a redistribution of moments at the section and an increase in the moment in the exterior girders. As the load was increased further, the interior girders failed in shear, and the test was terminated.

Bridge 3—This bridge, designed in 1937 for the equivalent of an H-15 loading, had the highest capacity of any of the other bridges tested. It behaved elastically up to very high loads, and it was not obvious when yielding first occurred. The reason for the absence of a clearly defined yield load is related to the stress-strain curve for the steel (Fig. 2), which indicates a very short yield plateau. Yielding did not occur simultaneously in all steel bars in all members at a cross section. The strain in the most highly stressed bars would increase to the strain-hardening region while other bars were reaching yield. This continuing process resulted in the behavior shown in Figure 5.

Bridge 4—The load-deflection curve for this bridge closely resembles that for a typical intermediate grade of structural steel, which is not surprising in view of the fact that the bridge was a noncomposite steel girder type. The stiffness of the bridge up to yield was considerably greater than that predicted for a noncomposite bridge because partial composite action existed up to yield. Failure of the bridge was initiated by yielding at the section of maximum positive moment. After this occurrence there followed considerable rotation of the resulting plastic hinge and very large deflections with only a nominal increase in load. Then plastic hinges formed near the 2 piers on the sides away from the loaded center span, and further deflection took place with a reduction in load capacity.

Ultimate Loads

The ultimate loads obtained from the field tests and the centerline deflection at ultimate load are given in Table 2.

COMPARISON OF RESULTS

Ultimate Loads

A comparison of calculated and measured ultimate loads is shown in Figure 7.

Theoretical Method—For all bridges except bridge 2 the theoretical method described earlier predicted within 9 percent the ultimate capacity of each bridge. The value predicted for bridge 2 was significantly higher than the measured value because of the loss of composite action in the interior girders at a load less than ultimate. The mode of failure for each bridge, again with the exception of bridge 2, was the same as that predicted. Redistribution of moments occurred in continuous bridges 1 and 4, and a limit analysis predicted the ultimate capacity very closely. The fact that the predicted ca-

pacity of bridge 4 was some 9 percent larger than the actual capacity was due, probably, to the eccentric placement of loads. This placement resulted in a rather uneven lateral distribution of load, with the likelihood that all 4 girders were unable to attain their maximum moment capacities simultaneously.

AASHO Specifications—The ultimate loads predicted by the AASHO Specifications were, in all cases, less than those measured. For bridges 1 and 4 the reason for the relatively low value predicted by AASHO Specifications is the fact that no redistribution of moments at ultimate load was considered. The ultimate load was calculated as that which produced ultimate moment at the section of maximum moment. The reason that the ultimate load calculated by using AASHO Specifications for bridge 3 was much lower than the measured value is due, most likely, to the fact that the maximum steel stress was taken as that at yield. Actually, because of the short yield plateau for the steel and the fact that a low percentage of steel was used, the steel stress at ultimate was much above yield.

Load at First Permanent Set

The load causing first permanent deflection set is not a clearly defined quantity, from either a theoretical or an experimental viewpoint. The computed values for this load were based on first yielding of steel. The measured values were taken from load-deflection curves for each bridge, and the load selected was that at which there was a definite deviation from a straight line. Computed and measured values for bridges 1, 3, and 4 are given in Table 2. No attempt was made to identify this load for prestressed concrete bridge 2. The computed loads for bridges 1 and 3 are somewhat higher than the load taken from load-deflection curves; however, the measured permanent deflection at a load equal to the computed load was approximately $\frac{1}{4}$ in. for bridge 1 and $\frac{1}{8}$ in. for bridge 3. Thus, the computed load causing first permanent set can be considered reasonable. The computed load for bridge 4 was approximately 75 percent of the measured load. This difference is most likely due to the fact that some degree of composite action did exist up to first yield, and the computations were based on the noncomposite behavior of the bridge.

CONCLUSIONS

The comparison of computed and experimentally determined results presented in this paper permits the following conclusions to be drawn:

1. The ultimate capacity of each bridge was computed on the basis of using material properties experimentally determined, considering an entire bridge to act as a wide beam spanning between supports, using a strain-compatibility method to determine ultimate moments, and taking account of redistribution of moments in continuous bridges 1 and 4. The ultimate capacities calculated in this manner agreed quite closely with the values obtained through field testing. The close agreement indicated that, as the load on a bridge is increased beyond first yielding, the more heavily loaded interior girders begin to yield, and additional load is taken by the exterior girders. Finally, near ultimate load, each girder is stressed approximately to its ultimate capacity, and the total bridge capacity approaches that obtained by considering the bridge to act as a wide beam, with the entire cross section including curbs acting as an integral unit.
2. The ultimate capacity of each bridge was also calculated on the basis of AASHO Specifications; specified nominal values for steel strengths were used. The loads obtained in this manner did not compare as closely with the actual ultimate bridge capacities as those calculated by the more exact method described earlier. However, design use of the more exact method is impractical. Thus, it is important to note that the calculations based on AASHO Specifications give a lower bound to the actual ultimate capacity of each of the 4 bridges tested.
3. The definition and experimental determination are somewhat less clear for load causing first permanent set than for ultimate load capacity. However, it appears from the tests and calculations that the method given in the AASHO Specifications for limiting overload on the basis of first permanent set is reasonable.

ACKNOWLEDGMENTS

Appreciation is expressed to the Tennessee Department of Highways for help in numerous ways during the conducting of the research described in this paper. Also, appreciation is expressed to the Tennessee Valley Authority for consistent cooperation. Finally, the advice, encouragement, and assistance given by Robert Varney and his co-workers at the Federal Highway Administration are gratefully acknowledged. The opinions, findings, and conclusions expressed in this paper are those of the authors and not necessarily those of the state or the Federal Highway Administration.

REFERENCES

1. Burdette, E. G., and Goodpasture, D. W. Final Report for Full-Scale Bridge Testing. Submitted to Tennessee Department of Highways and Federal Highway Administration, Dec. 31, 1971.
2. 1971 Interim Specifications. Committee on Bridges and Structures, American Association of State Highway Officials.
3. Building Code Requirements for Reinforced Concrete. American Concrete Institute, ACI 318-63.
4. Warwaruk, J., Sozen, M. A., and Siess, C. P. Investigation of Prestressed Reinforced Concrete for Highway Bridges: Part III—Strength and Behavior in Flexure of Prestressed Concrete Beams. Eng. Exp. Station, Univ. of Illinois, Bull. 464, 1962.
5. Khachaturian, N., and Gurfinkel, G. Prestressed Concrete, McGraw-Hill, 1969.